Title

Endothelin-1 Induces a Glycolytic Switch in Pulmonary Arterial Endothelial Cells via the Mitochondrial Translocation of Endothelial Nitric Oxide Synthase

Journal

American Journal of Respiratory Cell and Molecular Biology, 50(6)

ISSN

1044-1549

Authors

Sun, Xutong
Kumar, Sanjiv
Sharma, Shruti
et al.

Publication Date

2014-06-01

DOI

10.1165/rcmb.2013-0187oc

Peer reviewed

ORIGINAL RESEARCH

Endothelin-1 Induces a Glycolytic Switch in Pulmonary Arterial Endothelial Cells via the Mitochondrial Translocation of Endothelial Nitric Oxide Synthase

Xutong Sun[1]*, Sanjiv Kumar[1]*, Shruti Sharma[1]*, Saurabh Aggarwal[1], Qing Lu[1], Christine Gross[1], Olga Rafikova[1], Sung Gon Lee[1], Sridevi Dasarathy[1], Yali Hou[1], Mary Louise Meadows[1], Weihong Han[2], Yunchao Su[2], Jeffrey R. Fineman[3,4], and Stephen M. Black[1]

[1]Pulmonary Disease Program, Vascular Biology Center, and [2]Department of Pharmacology & Toxicology, Georgia Regents University, Augusta, Georgia; and [3]Department of Pediatrics and [4]the Cardiovascular Research Institute, University of California San Francisco, San Francisco, California

Abstract

Recent studies have indicated that, during the development of pulmonary hypertension (PH), there is a switch from oxidative phosphorylation to glycolysis in the pulmonary endothelium. However, the mechanisms underlying this phenomenon have not been elucidated. Endothelin (ET)-1, an endothelial-derived vasoconstrictor peptide, is increased in PH, and has been shown to play an important role in the oxidative stress associated with PH. Thus, in this study, we investigated whether there was a potential link between increases in ET-1 and mitochondrial remodeling. Our data indicate that ET-1 induces the redistribution of endothelial nitric oxide synthase (eNOS) from the plasma membrane to the mitochondria in pulmonary arterial endothelial cells, and that this was dependent on eNOS uncoupling. We also found that ET-1 disturbed carnitine metabolism, resulting in the attenuation of mitochondrial bioenergetics. However, ATP levels were unchanged due to a compensatory increase in glycolysis. Further mechanistic investigations demonstrated that ET-1 mediated the redistribution of eNOS via the phosphorylation of eNOS at Thr495 by protein kinase C δ. In addition, the glycolytic switch appeared to be dependent on mitochondrial-derived reactive oxygen species that led to the activation of hypoxia-inducible factor signaling. Finally, the cell culture data were confirmed *in vivo* using the monocrotaline rat model of PH. Thus, we conclude that ET-1 induces a glycolytic switch in pulmonary arterial endothelial cells via the redistribution of uncoupled eNOS to the mitochondria, and that preventing this event may be an approach for the treatment of PH.

Keywords: mitochondrial bioenergetics; endothelial nitric oxide synthase uncoupling; protein kinase C δ; peroxynitrite; superoxide

Clinical Relevance

It is becoming increasingly clear that the Warburg effect plays an important role in the development of pulmonary hypertension (PH). However, mechanisms underlying the glycolytic switch are unresolved. Our data demonstrate that endothelin-1, which is increased in PH, is capable of inducing aerobic glycolysis in pulmonary endothelial cells.

Mitochondria are essential for energy metabolism through their ability to generate cellular ATP through oxidative phosphorylation. Increasing evidence suggests that mitochondrial remodeling is a critical event in a number of cardiovascular diseases, including pulmonary hypertension (PH) (1, 2). PH is a fatal disease characterized by pathologic vascular remodeling, which eventually leads to right ventricular failure and death. Several decades ago, Warburg (3) identified

(Received in original form April 24, 2013; accepted in final form December 11, 2013)

*These authors contributed equally.

This work was supported in part by National Institutes of Health grants HL60190 (S.M.B.), HL67841 (S.M.B.), P01HL0101902 (S.M.B.), HD039110 (S.M.B.), and HL61284 (J.R.F.), by National Affiliates of the American Heart Association Scientist Development Grant 11SDG7460024 (S.S.), and Cardiovascular Discovery Institute Seed Awards (S.S. and S.K.). C.M.G. was funded in part by American Heart Association predoctoral fellowship award 12PRE12060224. O.R. was funded in part by National Institutes of Health postdoctoral fellowship award F32HL103136.

Correspondence and requests for reprints should be addressed to Stephen M. Black, Ph.D., Vascular Biology Center: CB-3211B, Georgia Regents University, 1459 Laney Walker Blvd, Augusta, GA 30912. E-mail: sblack@georgiahealth.edu

This article has an online supplement, which is accessible from this issue's table of contents at www.atsjournals.org

Am J Respir Cell Mol Biol Vol 50, Iss 6, pp 1084–1095, Jun 2014

Originally Published in Press as DOI: 10.1165/rcmb.2013-0187OC on January 6, 2014
Internet address: www.atsjournals.org

a metabolic switch to aerobic glycolysis in cancer cells (i.e., the "Warburg effect"). Recent evidence has suggested that, like cancer, there is a switch from oxidative phosphorylation to glycolysis in the pulmonary arterial endothelial cells (PAECs) during the development of PH (4). Nitric oxide (NO) levels are lower in patients with idiopathic pulmonary arterial hypertension compared with healthy control subjects (4). Accumulating evidence suggests that decreased NO production and reduced mitochondrial function, coupled to increased glycolysis, seem to be consistent markers of PH across multiple species, including rodents and humans (4). However, the mechanisms underlying this phenomenon have not been well characterized.

Endothelin (ET)-1 is a potent endogenous vasoconstrictor that is highly expressed in the lungs of patients with PH (5). Increased levels of ET-1 are involved in the oxidative stress associated with PH (6). Our recent studies indicate that inhibition of ET-1 signaling significantly attenuates the oxidative and nitrosative stress associated with PH (7). We have also shown that acute increases in pulmonary blood flow (PBF) are followed by a compensatory pulmonary vascular constriction, which is mediated by an ET-1–dependent decrease in endothelial NO synthase (eNOS) activity (8). Furthermore, acute increases in PBF are limited by an ET-1–dependent decrease in NO production via alterations in eNOS phosphorylation (9). Thus, the purpose of this study was to determine if there was a mechanistic link between increased ET-1, decreases in NO signaling, and alterations in mitochondrial bioenergetics in PAECs and in a rat model of PH induced by single-dose administration of monocrotaline (MCT).

In cultured PAECs, we found that ET-1 induces eNOS uncoupling and the translocation of eNOS to the mitochondria. This resulted in the perturbation of carnitine metabolism and attenuated mitochondrial bioenergetics. We also found that the balance of ATP generation under ET-1 treatment was shifted from oxidative phosphorylation to glycolysis. In addition, mechanistic investigations indicated that ET-1–induced eNOS mitochondrial redistribution and the disruption of mitochondrial bioenergetics occurs via protein kinase (PK) C δ–mediated phosphorylation of eNOS at Thr495, a threonine residue within the calmodulin-binding domain. Furthermore, our data indicate that the glycolytic switch was induced via the reactive oxygen species (ROS)-mediated activation of hypoxia-inducible factor (HIF). Finally, we found that the changes in PAECs were mirrored in the MCT-rat model of PH.

Materials and Methods

Animals

Animals used in this study are described in the online supplement. All experimental procedures were approved by the Institutional Animal Care and Use Committee of Georgia Regents University.

Measurement of Right Ventricle Thickness

Measurement of right ventricle (RV) thickness is described in the online supplement.

Antibodies and Chemicals

Antibodies and chemicals used in this study are described in detail in the online supplement.

Cell Culture and Treatment

Ovine PAECs were isolated as described previously (10). Cells were maintained and treated as described in the online supplement, and used between passages 8 and 12.

Western Blot Analysis

This is described in detail in the online supplement.

Immunoprecipitation Analysis

The interaction of eNOS with PKCδ was determined by immunoprecipitation analysis as previously described (9). The efficiency of immunoprecipitation was normalized by reprobing the membranes with the immunoprecipitation antibody (eNOS).

Inhibition of PKCδ

Inhibition of PKCδ is described in the online supplement.

In Vitro Interaction of PKCδ and eNOS.

In Vitro interaction of PKCδ and eNOS is described in the online supplement.

Mitochondrial Isolation

Mitochondrial isolation is described in detail in the online supplement.

Measurement of Superoxide Levels

To detect superoxide generation, electron paramagnetic resonance measurements were performed using the spin trap, 1-hydroxy-3-methoxycarbonyl-2,2,5,5-tetramethylpyrrolidine.HCl (20 μM in Dulbecco's phosphate-buffered saline + 25 μM desferrioxamine; Enzo Life Sciences, La Jolla, CA), as we have described previously (11). NOS-derived superoxide levels were determined by subtracting the superoxide values in the presence of the NOS inhibitor, ethylisothiourea (100 μM; Tocris, Ellisville, MO) from the superoxide values in the absence of ethylisothiourea.

Measurement of Peroxynitrite Levels in Cells

The formation of peroxynitrite was determined using the oxidation of dihydrorhodamine (DHR) 123 (EMD Millipore, Billerica, MA) to rhodamine 123 in the presence of polyethylene glycol–catalase (100 U, 30 min), as previously described (12).

Determination of Total Protein Nitration

To examine global protein nitration, cell or tissue lysates were analyzed for 3-nitrotyrosine levels using a dot blot procedure as previously described (12).

Live Cell Imaging of eNOS Redistribution to the Mitochondria

Live cell imaging of eNOS redistribution to the mitochondria is described in detail in the online supplement.

Determination of Mitochondrial Superoxide Levels

Determination of mitochondrial superoxide levels is described in detail in the online supplement.

Analysis of Mitochondrial Membrane Potential

Mitochondrial membrane potential was estimated using the lipophilic cation 5,5′6,6′-tetrachloro-1,1′,3,3′-tetraethyl benzimidazolyl carbocyanine iodide (Trevegin, Gaithersburg, MD), as previously described (13).

Quantification of Total and Free Carnitine Levels by HPLC

Quantification of total and free carnitine levels by HPLC was performed as previously described (14) and detailed in the online supplement.

Analysis of Mitochondrial Bioenergetics

Analysis of mitochondrial bioenergetics is described in detail in the online supplement.

Analysis of Cellular Glycolysis

Analysis of cellular glycolysis is described in the online supplement.

Determination of ATP Levels

Determination of ATP levels is described in the online supplement

Analysis of HIF-1 Activity

Analysis of HIF-1 activity is described in the online supplement.

Measurement of ET-1 Levels

Measurement of ET-1 levels is described in the online supplement.

Cell Proliferation Assay

At 24 hours after transient transfection with prepro-ET-1 or green fluorescent protein (GFP) (as a control), cells were trypsinized, resuspended in culture medium, and 5×10^4 cells seeded in 24-well plates. Cell numbers were then quantified using MoxiZ (ORFLO Technologies, Hailey, ID) every 24 hours for 5 days.

Cell Apoptosis Assay

The cell apoptosis assay is described in the online supplement.

Statistical Analysis

The statistical analysis is described in the online supplement.

Results

ET-1 Induces Mitochondrial Dysfunction in PAECs

Increased mitochondrial superoxide generation (15) and disturbed mitochondrial membrane potential (15) are considered to be hallmarks of mitochondrial dysfunction. By measuring changes in MitoSOX red fluorescence, we examined the effect of ET-1 on mitochondrial superoxide levels. Exposure of cells to 100 nM ET-1 caused a significant increase in MitoSOX fluorescence (Figure 1A). Changes in mitochondrial membrane potential were analyzed using the lipophilic cation, 5,5′6,6′-tetrachloro-1,1′,3,3′-tetraethyl benzimidazolyl carbocyanine iodide. ET-1 caused a significant decrease in DePsipher red fluorescence (Figure 1B), indicating a loss of mitochondrial membrane potential. Furthermore, we found that these changes correlated with a loss of carnitine homeostasis, as determined by increases in the levels of acyl carnitines (Figure 1C) and the disruption of the acyl carnitine:free carnitine ratio (Figure 1D).

ET-1 Disrupts Mitochondrial Bioenergetics and Induces Glycolytic Switch in PAECs

Carnitine homeostasis is critical for maintaining normal mitochondrial function, and we have shown that its disruption is associated with alterations in mitochondrial bioenergetics (16). Using the Seahorse XF24 Analyzer (North Billerica, MA), we examined the effect of ET-1 on mitochondrial bioenergetics in PAECs. Our data indicate that, although basal respiration was unaffected (Figure 2A), both the reserve (Figure 2B) and maximal (Figure 2C) respiratory capacities were significantly reduced by ET-1. Surprisingly, the disruption of mitochondrial bioenergetics did not significantly change cellular ATP levels (Figure 2D), suggesting that there was a compensatory increase in glycolysis. To test this, we again used the Seahorse XF24 Analyzer. Our data also indicate that basal glycolytic rate (Figure 2E), and maximal (Figure 2F) and spare (Figure 2G) capacities, are all significantly increased by exposure to ET-1.

ET-1 Induces the Mitochondrial Translocation of eNOS in PAECs

Our recent studies indicate that asymmetric dimethylarginine (ADMA) disrupts mitochondrial bioenergetics in PAECs due to eNOS uncoupling secondary to a redistribution of eNOS from the plasma membrane to the mitochondria (16). Thus, we next evaluated the effect of ET-1 on eNOS uncoupling. We found that ET-1 (100 nM, 4 h) significantly increased NOS-derived superoxide (Figure 3A). NO and superoxide can interact to produce highly reactive peroxynitrite ($ONOO^-$) (17). Thus, we next measured the oxidation

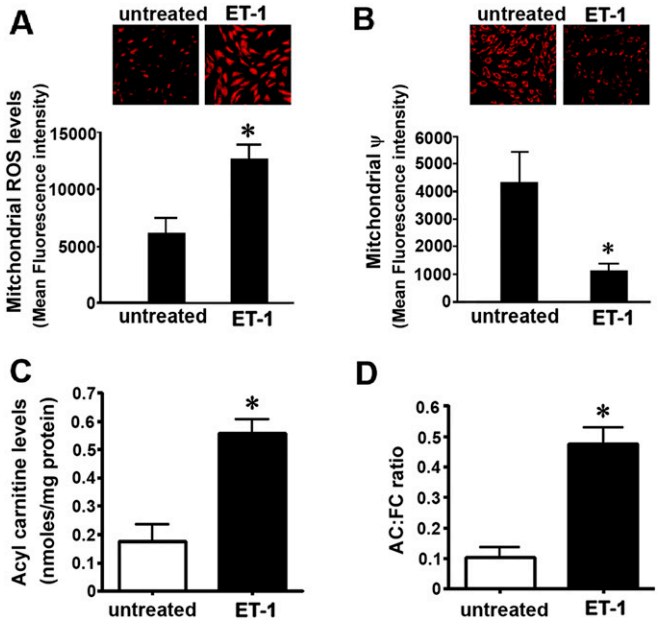

Figure 1. Endothelin (ET) 1 disrupts mitochondrial function in pulmonary arterial endothelial cells (PAECs). PAECs were treated with ET-1 (100 nM, 4 h) and mitochondrial superoxide levels were determined using the MitoSOX Red mitochondrial superoxide indicator (*A*). ET-1 increases mitochondrial reactive oxygen species (ROS) generation in PAECs (*A*). ET-1 also reduces the mitochondrial membrane potential, as estimated by the decrease in aggregated red form of the DePsipher compound (*B*). ET-1 also significantly increases acylcarnitine levels (*C*) and the acylcarnitine:free carnitine ratio (*D*) in PAECs. Values are means ± SEM; $n = 4$–8. *$P < 0.05$ versus untreated. AC, acylated carnitine; FC, free carnitine.

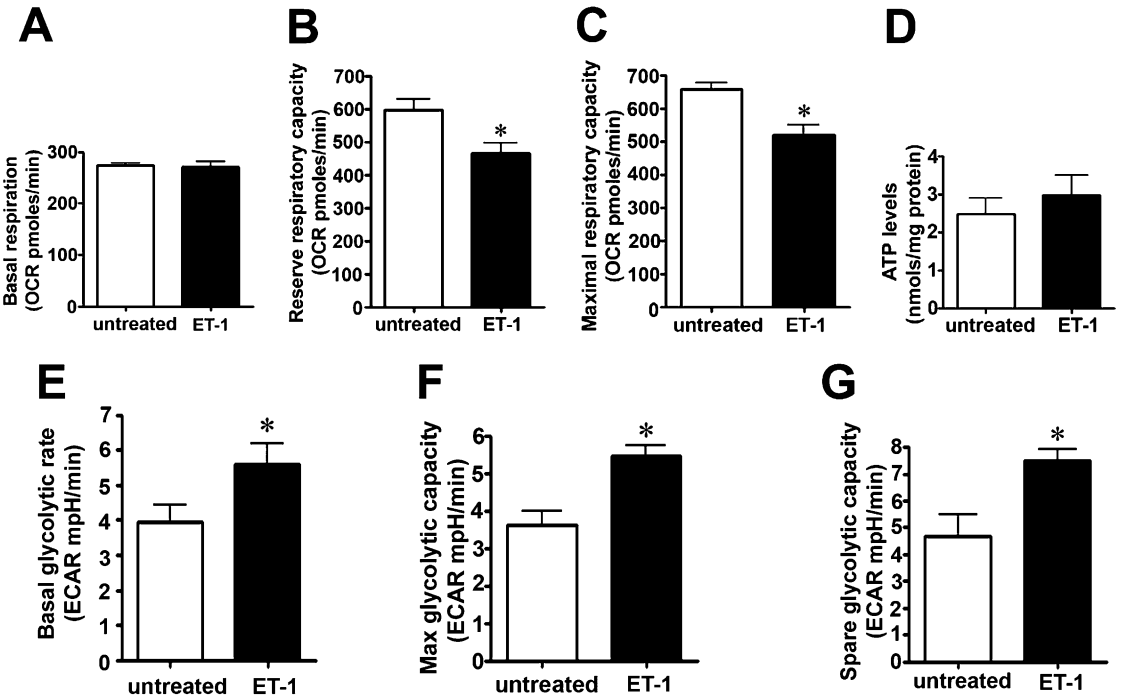

Figure 2. ET-1 induces a glycolytic switch in PAECs. PAECs (75,000 cells/0.32 cm^2) were exposed to ET-1 (100 nM, 4 h), then the Seahorse XF24 analyzer was used to measure changes in oxygen consumption rate (OCR). Oligomycin (1 μM), p-triflouromethoxyphenylhydrazone (1 μM), and rotenone and antimycin A (1 μM each) were added sequentially. ET-1 did not significantly alter basal mitochondrial respiration (*A*). However, both the reserve respiratory capacity (*B*) and the maximal respiratory capacity (*C*) in PAECs were significantly attenuated by ET-1. ET-1 did not significantly alter ATP levels (*D*). The basal glycolytic rate (*E*), and the maximum (*F*) and spare (*G*) glycolytic capacities, were significantly increased by ET-1. Values are means ± SEM; n = 6–12. *$P < 0.05$ versus untreated. ECAR, extracellular acidification rate; mpH, milli-pH units.

of DHR123 to estimate changes in $ONOOO^-$. We found that ET-1 (100 nM, 4 h) significantly enhanced $OONOO^-$-dependent DHR123 oxidation (Figure 3B) and total protein nitration levels (Figure 3C). Furthermore, our data indicate that ET-1 induces the mitochondrial redistribution of eNOS in PAECs (Figure 3D). To confirm this result, and to determine if the translocation was $ONOO^-$ dependent, PAECs were transiently transfected with an eNOS–GFP construct (18), treated with MitoTracker (Thermo Fisher Scientific Inc., Waltham, MA), and then exposed to ET-1 in the presence or absence of the cell-permeant superoxide dismutase mimetic, manganese(III) tetrakis (1-methyl-4-pyridyl)porphyrin (MnTMPyP). The colocalization of the GFP-tagged eNOS with the red-labeled mitochondria was determined over a 90-minute period, and the Pearson product-moment correlation coefficient determined to estimate the redistribution of eNOS to the mitochondria. ET-1 induced a time-dependent increase in the localization of eNOS to the mitochondria (Figure 3E), whereas MnTMPyP attenuated this redistribution (Figure 3E), indicating the requirement for $ONOO^-$. However, unlike our previous studies, in which ADMA-mediated eNOS mitochondrial translocation was dependent on Akt-1–mediated phosphorylation of eNOS at S1177 and S617 (19), ET-1 actually decreased both pS1177- (Figure 3F) and pS617-eNOS (Figure 3G) levels in PAECs. Akt activity itself was unchanged, as estimated by measuring p473-Akt1 levels (Figure 3H). Together, these data suggest that other mechanisms are involved in the mitochondrial redistribution of eNOS in PAECs exposed to ET-1.

ET-1 Induces the Mitochondrial Redistribution of eNOS via PKCδ-Mediated Phosphorylation of eNOS at Thr495

Our recent studies have shown that PKCδ can phosphorylate eNOS at T495 (9), whereas others have shown that T495 phosphorylation can induce eNOS uncoupling (20). Thus, to further investigate the mechanism of ET-1–induced eNOS mitochondrial redistribution, we first examined the effect of ET-1 on eNOS phosphorylation at T495 (pT495). We found that the levels of pT495 eNOS are significantly increased in the presence of ET-1 (Figure 4A), and this correlated with an increase in the interaction of eNOS with PKCδ (Figure 4 B). We next incubated recombinant human eNOS purified from *Escherichia coli* (21) with recombinant PKCδ in the presence of ATP and kinase buffer. Western blotting was then used to confirm eNOS phosphorlation at T495 (Figure 4C). In addition, a PKCδ-inhibitory peptide significantly attenuated the ability of ET-1 to increase the redistribution of eNOS to the mitochondria (Figures 4D and 4E). Furthermore, although we found no changes in basal respiration (Figure 4F), the ET-1–mediated reduction in the spare (Figure 4G) and maximal (Figure 4H) respiratory capacity was attenuated in the presence of the PKCδ inhibitory peptide. Interestingly, we found that the PKCδ-inhibitory peptide, either alone or in the presence of ET-1, increased the spare and maximal respiratory capacity in PAECs (Figures 4G and 4H).

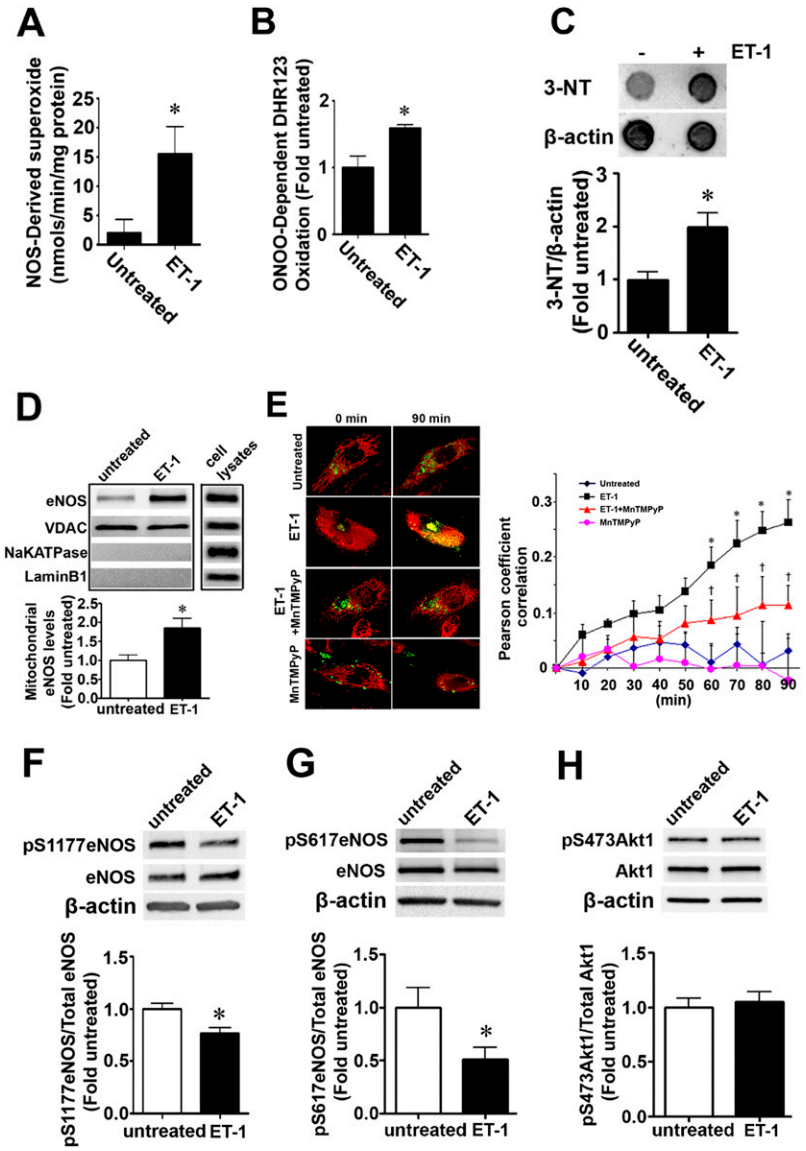

Figure 3. ET-1 induces the mitochondrial redistribution of endothelial nitric oxide (NO) synthase (eNOS) in PAECs. PAECs were exposed to ET-1 (100 nM) for 4 hours, and the effect on NOS-derived superoxide and peroxynitrite levels were determined. ET-1 increases NOS-derived superoxide levels (*A*), peroxynitrite levels (*B*), and total protein nitration levels (*C*). Mitochondrial protein extracts (5 μg) were subjected to Western blotting using an antibody raised against eNOS. ET-1 increases eNOS accumulation in the mitochondria (*D*). Loading was normalized by reprobing with the mitochondrial protein, voltage-dependent anion channel (VDAC), and reprobed with antibodies raised against NaKATPase, or laminB1, to demonstrate no cross-contamination with the plasma membrane, or nuclear fractions, respectively. A separate gel was run using a PAEC lysate (20 μg) to demonstrate that each antibody recognizes the ovine protein (*D*). PAECs were also transiently transfected with an eNOS construct tagged with green fluorescent protein (GFP). The mitochondria were labeled with MitoTracker (*red*) and the cells pretreated or not with manganese(III) tetrakis(1-methyl-4-pyridyl)porphyrin (MnTMPyP) (25 μM, 20 min) followed ET-1 (100 nM). The extent of mitochondrial localization of eNOS was then determined by measuring the intensity of yellow fluorescence (overlap of red fluorescence of MitoTracker and green fluorescence of eNOS–GFP). There was a time-dependent increase in yellow fluorescence in the ET-1–treated cells, and this was blocked by the presence of MnTMPyP (*E*). In addition, Western blotting demonstrated that that ET-1 (100 nM, 4 h) significantly decreased the phosphorylation of eNOS at both S1177 (*F*) and S617 (*G*), although there were no changes identified in Akt1 activity, as estimated by measuring changes in the levels of p473-Akt1 (*H*). Values are means ± SEM; $n = 4$–12. $^{*}P < 0.05$ versus untreated; $^{\dagger}P < 0.05$ versus ET-1 alone. 3-NT, 3-nitrotyrosine.

Overexpression of a Phospho-T495eNOS Mimic Disrupts Mitochondrial Bioenergetics in PAECs

To confirm that eNOS phosphorylation at T495 is involved in ET-1–mediated disruption of mitochondrial bioenergetics, we used an adenoviral construct to overexpress a T495D-eNOS mutant protein. We found that the overexpression of the T495D-eNOS protein in PAECs (Figure 5A) increased both NOS-derived superoxide (Figure 5B) and $ONOO^{-}$ levels (Figure 5C). In addition, the introduction of an aspartic acid at T495 in the eNOS–GFP construct, to mimic the negative charge associated with phosphorylation, significantly increased the redistribution of eNOS to the mitochondria (Figure 5D). Moreover, the increase in ROS generation was associated with a reduction in basal respiration (Figure 5E), the amount of oxygen consumed for ATP generation (Figure 5F), and both the reserve (Figure 5G) and maximal (Figure 5H) respiratory capacities.

ET-1 Induces Glycolysis in PAECs via ROS-Mediated HIF-1 Activation

To further examine the mechanism of the ET-1–mediated glycolytic shift, we examined the role of mitochondrial-derived ROS. We found that the mitochondrial-targeted antioxidant, MitoQ, decreased both control and ET-1–induced mitochondrial ROS generation in PAECs (Figure 6A). Next, we determined the effect of ET-1 on HIF-1α promoter activity. Our results indicate that ET-1 significantly increased HIF-1 activity, as determined by an increase in promoter activity in an HIF-1–dependent promoter linked to luciferase (Figure 6B). Furthermore, the increase in HIF-1–dependent promoter activity was attenuated in the presence of MitoQ (Figure 6B), suggesting that mitochondrial ROS activates the HIF-1 signaling pathway. Furthermore, the overexpression of prepro-ET-1 (Figure 6C) increased the protein levels of HIF-1–dependent downstream target genes, enolase-2 (Figure 6D) and glucose-6-phosphate dehydrogenase (G6PD; Figure 6E), which are known to be involved in glycolysis (reviewed in Refs. 22, 23). Furthermore, prepro-ET-1 overexpression increased the proliferation of PAECs (Figure 6F) and enhanced their resistance

to TNF-α–mediated apoptosis (Figure 6G), mimicking the proproliferative, antiapoptotic phenotype associated with PH in humans (reviewed in Refs. 7, 24).

ET-1 Induces eNOS Mitochondrial Translocation and Enhances Glycolytic Protein Levels in Rodent Models of PH

One of the hallmarks of the development of PH is an increase in RV thickness (reviewed in Ref. 24). At Day 0 (before MCT injection) and 7, 14, 21, and 28 days post-MCT, we used ultrasound to determine when there was a significant increase in RV thickness. Our data determined that RV thickness was significantly increased 21 days after MCT injection (Figure 7A). Based on these data, we hypothesized that, if ET-1–mediated eNOS mitochondrial translocation was important in inducing the glycolytic switch associated with PH, then it should occur before 21 days. Accordingly, we performed subsequent studies using lung tissue isolated from rats exposed to MCT for 14 days. We first confirmed that ET-1 levels were significantly increased in MCT rats (Figure 7B). Subsequently, we found that 14 days of exposure to MCT significantly increased the levels of phosphor-PKCδ (Figure 7C), phosphor-T495eNOS (Figure 7D), NOS-derived superoxide (Figure 7E), and total protein nitration (Figure 7F) levels. Furthermore, mitochondrial eNOS protein levels were also increased (Figure 7G). Next, we re-examined our rat model to determine if the changes in eNOS mitochondrial translocation were attributable to the same HIF-1–glycolysis pathway that we observed in cultured PAECs. Our data indicate that HIF-1α protein levels are increased in MCT rats (Figure 7H), and this correlates with an increase in enolase-2 (Figure 7I) and G6PD (Figure 7J) protein levels. To further confirm the importance of this signaling pathway, we also examined a mouse model of PH induced by exposure to chronic hypoxia. Consistent with the results in MCT rats, increases in ET-1 (Figure 7K) correlate with increased phosphor-PKCδ (Figure 7L), and enhanced levels of mitochondrial eNOS (Figure 7M).

Discussion

Mitochondrial remodeling in cancer results in aerobic glycolysis, in which rapidly

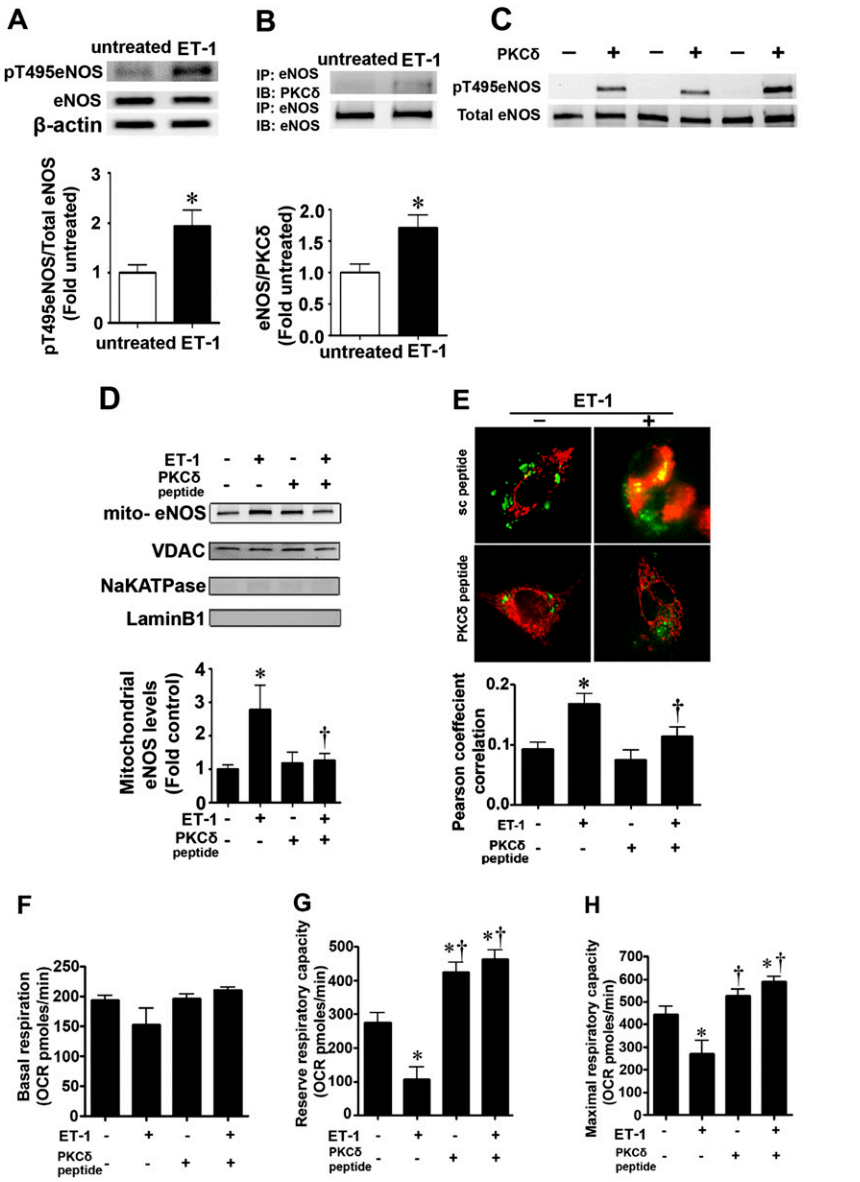

Figure 4. ET-1 treatment increases eNOS phosphorylation at Thr495 via protein kinase (PK) Cδ signaling, leading to the disruption of mitochondrial bioenergetics in PAECs. PAECs were exposed to ET-1 (100 nM, 4 h), whole-cell extracts (15 μg) were prepared, and immunoblots were performed using an antibody raised against pT495-eNOS (*A*). Loading was normalized by running a duplicate gel that was probed with an antibody raised against total eNOS (*A*). A representative image is shown. ET-1 significantly increases eNOS phosphorylation at T495 (*A*). Cell lysates (500 μg) were also subjected to immunoprecipitation (IP) using an antibody specific to eNOS, then analyzed by Western blot (IB) analysis using a specific antibody raised against PKCδ. A representative image is shown (*B*). Blots were stripped and reprobed for eNOS to normalize for the immunoprecipitation efficiency. Densitometric values were then obtained. ET-1 significantly increased the interaction of eNOS with PKCδ (*B*). Phosphorylation of eNOS at T495 was also induced *in vitro* when recombinant human eNOS was incubated with purified PKCδ (*C*). Cells were also pretreated with a PKCδ-inhibitory peptide or a scrambled (sc) peptide as a control for 1 hour, followed by ET-1 (100 nM, 4 h) treatment. Mitochondrial protein extracts (3 μg) were then prepared and subjected to Western blot analysis using an antibody raised against eNOS. ET-1 increased eNOS accumulation in the mitochondria (*D*). Loading was normalized by reprobing with the mitochondrial protein, VDAC (*D*). Cells were transfected with eNOS–GFP. After 48-hour transfection, the mitochondria were labeled with MitoTracker (*red*) and pretreated with a PKCδ-inhibitory peptide or an sc peptide as a control (1 μM each peptide for 1 h). The extent of mitochondrial localization of eNOS in the presence of ET-1

growing cells shift from oxidative phosphorylation to glycolysis to generate ATP, and so improve their survival (3). Increasing evidence indicates that aerobic glycolysis is not a unique characteristic of cancer cells, but is also found in other cell types, including T cells as they engage in rapid growth and proliferation (25). Furthermore, a number of studies have shown that mitochondrial dysfunction is associated with various pathologic conditions, including cancer (reviewed in Ref. 22), hypoxia–ischemic injuries (1), and PH (2). Recent studies have also shown that, during the development of PH, there is a switch from oxidative phosphorylation to glycolysis in both smooth muscle (26) and endothelial cells (4). However, the mechanisms underlying this phenomenon have not been elucidated. Here, we demonstrate that ET-1 attenuates mitochondrial bioenergetics while inducing aerobic glycolysis.

ET-1, a 21–amino acid peptide, plays an important role in the regulation of vascular function. An increase in ET-1 levels results in vasoconstriction and increased oxidative stress (7, 9). The induction of oxidative stress by ET-1 appears to be multifactorial. We have previously shown that ET-1 stimulates reduced nicotinamide adenine dinucleotide oxidase activity in vascular smooth muscle cell *in vitro* (27), whereas the increased levels of ET-1 induced by inhaled NO are associated with increased superoxide and peroxynitrite generation (8). However, the role of ET-1 in increasing mitochondrial ROS is less certain. Emerging evidence suggests that ET-1 increases mitochondrial ROS production in cardiomyocytes (28). Studies have also shown that ET-1 can stimulate mitochondrial ROS generation in vascular smooth muscle cells through the elevation of mitochondrial calcium levels (28). However, in endothelial cells, there is only indirect evidence that ET-1 can increase mitochondrial ROS. For example, the combined metabolic burden of homocysteine and high glucose stimulates ET-1 synthesis in bovine aortic endothelial cells via a mechanism dependent on the production of mitochondrial ROS (29). Furthermore, in human aortic endothelial cells, uncoupling protein 2 overexpression decreases ET-1 mRNA expression and prevents the disruption of the mitochondrial membrane potential induced by lysophophatidylcholine (30). Prior studies have also shown that ET-1 is associated with disturbed mitochondrial bioenergetics in cultured rat cardiomyocytes (31). In cultured cardiomyocytes treated with a mitochondrial inhibitor, ET-1 mRNA was markedly increased, which correlated with increases in glycolysis (32). We also found that ET-1 decreased both reserve and maximal respiratory capacity in PAECs, and that an increased glycolytic rate acted as a compensatory source for ATP generation.

In our studies, we found that ET-1 increased mitochondrial ROS generation and disrupted the mitochondrial membrane potential, all of which correlated with the disruption of carnitine homeostasis. Carnitine homeostasis plays an important role in regulating β oxidation of small- and medium-chain fatty acids in cells, and we have previously shown that carnitine homeostasis is disrupted in our lamb model of pulmonary endothelial dysfunction associated with increased PBF (14). Furthermore, this correlates with an increase in lactate levels (14), suggesting that a glycolytic switch may also be induced in these lambs. Interestingly, these lambs also have decreased ATP levels (16), suggesting that the glycolytic switch is unable to maintain ATP demand. We did not observe a decrease in ATP in PAECs exposed to ET-1, nor have reductions in ATP been observed in PAECs isolated from patients with idiopathic pulmonary arterial hypertension (33). This suggests that there are compensatory mechanisms that are induced during advanced disease that restore ATP levels, or that there are differences between pediatric and adult forms of PH. In addition, although ET-1 increased basal glycolysis, basal respiration was unaffected, despite a decrease in mitochondrial membrane potential. Although we do not have a definitive answer as to why this occurs, there is precedence in the literature for this to occur. For example, Darley-Usmar's group (34) have shown that that the exposure of bovine aortic endothelial cells to NO or hydrogen peroxide had little impact on basal mitochondrial function, but that both treatments decreased mitochondrial reserve capacity. In addition, although mitochondrial membrane potential is generally related to mitochondrial respiration, they are not necessarily correlated, especially when one compares mitochondrial membrane potential to basal mitochondrial respiration. For example, a recently published study has shown that, in phosphatase and tensin homolog-induced kinase 1 knockout mouse fibrolasts, the basal mitochondrial respiration is increased, whereas maximum respiration and spare respiratory capacity are decreased, as is the membrane potential (35).

Our data also show that the disruption of carnitine homeostasis and mitochondrial bioenergetics in PAECs exposed to ET-1 correlates with the mitochondrial redistribution of eNOS. This is in agreement with our recent studies in which we showed that asymmetric ADMA, an endogenous NOS uncoupler, induces eNOS mitochondrial redistribution and the disruption of mitochondrial bioenergetics through the nitration of carnitine acetyl transferase and the attenuation of carnitine homeostasis (16). However, ADMA induces eNOS mitochondrial translocation via the nitration-mediated activation of Akt1 and increased phosphorylation of eNOS at S617 and S1,177 (19). Interestingly, although the ET-1–dependent translocation of eNOS is dependent on uncoupled eNOS, it appears to be independent of Akt-1 signaling, as we observed no increase in Akt-1 activity and a reduction in eNOS phosphorylation at S617 and S1,177. The reason for this discrepancy is unclear. It is likely that, in both cases, mitochondrial translocation is dependent on the mitochondrial targeting sequence previously identified in eNOS (36). Our prior molecular modeling studies have

Figure 4. (Continued). (100 nM, 60 min) was then determined by measuring the intensity of yellow fluorescence (overlap of red fluorescence of MitoTracker and green fluorescence of eNOS–GFP) (*E*). The PKCδ-inhibitory peptide significantly reduced the eNOS mitochondrial redistribution induced by ET-1 (*E*). PAECs (75,000 cells/0.32 cm^2) were exposed to ET-1 (100 nM, 4 h). The PKCδ-inhibitory peptide, or an sc peptide as a control (1 μM each peptide), were added for the last 2 hours of the experiment. The Seahorse XF24 analyzer was used to measure changes in OCR. Although the PKCδ-inhibitory peptide did not change basal respiration (*F*), it completely abolished the ET-1–mediated reduction in both reserve (*G*) and maximal (*H*) respiratory capacity. Values are means ± SEM; $n = 3$–10. $^{*}P < 0.05$ versus untreated; $^{\dagger}P < 0.05$ versus ET-1 with sc peptide.

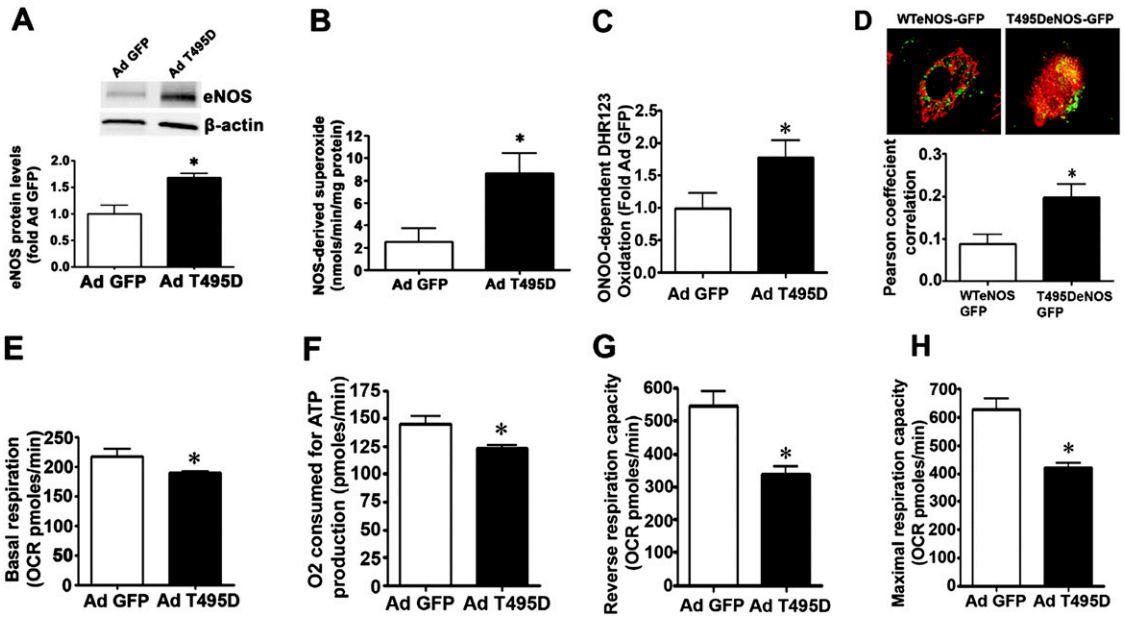

Figure 5. eNOS phosphorylation at Thr495 triggers eNOS uncoupling and the reduction in mitochondrial bioenergetics in PAECs. PAECs were transduced with adenoviral constructs for GFP (AdGFP) or mutant eNOS (AdT495DeNOS). After 48 hours, the cells were harvested and immunoblots were performed on total lysates using an antibody raised against eNOS with loading normalized by reprobing the membranes with an antibody specific to β-actin (*A*). A representative image is shown. Transduction of AdT495DeNOS increases eNOS protein levels by roughly twofold (*A*). NOS-derived superoxide (*B*) and peroxynitrite levels (*C*) were both significantly increased in AdT495DeNOS-expressing cells. PAECs were also transiently transfected with wild-type eNOS–GFP or a T495DeNOS–GFP mutant. After 48 hours, the mitochondria were labeled with MitoTracker (*red*) and the extent of eNOS mitochondrial localization determined by measuring the intensity of yellow fluorescence (overlap of red fluorescence of MitoTracker and green fluorescence of eNOS–GFP) (*D*). The T495-eNOS protein is preferentially localized to the mitochondria (*D*). The Seahorse XF24 analyzer was used to measure changes in OCR. AdT495DeNOS overexpression significantly decreased basal OCR (*E*), the oxygen consumed for ATP production (*F*), and both reserve (*G*) and maximal (*H*) respiratory capacity. Values are means ± SEM; $n = 3–11$. $^*P < 0.05$ versus Ad-GFP.

suggested that the mitochondrial targeting sequence is normally located deep within the eNOS protein, and that the phosphorylation of S617 increases its solvent accessibility, causing it to flex outward, which increases its exposure to the unidentified protein(s) that shepherd it to the mitochondria (19). Thus, it is possible that the phosphorylation at T495 that we have observed when PAECs are exposed to ET-1 also increases the exposure of the mitochondrial targeting sequence. We also found that MnTMPyP significantly attenuated ET-1–induced eNOS mitochondrial redistribution, which supports our prior work demonstrating that eNOS mitochondrial translocation in PAECs is enhanced by nitrative stress (19). Thus, it is possible that the increase in peroxynitrite formed when eNOS uncouples is inducing its nitration, and that this could also increase the exposure of the mitochondrial targeting sequence. Indeed we have shown that there are two nitration sites in eNOS, located at Y608 and Y666, that flank the mitochondrial targeting sequence located between aa627 and aa631 in eNOS (36). However, further studies will be required to test these possibilities.

It is clear that NOS uncoupling is a complex process regulated by decreases in the availability of the substrate, L-arginine, the cofactor, tetrahydrobiopterin, or, as we have recently shown, increases in the cellular levels of ADMA (37). Studies indicate that PKC-mediated eNOS phosphorylation at T495, a negative regulatory site, is associated with eNOS uncoupling (20). Consistent with these studies, here we have shown that ET-1 induces the binding by eNOS to PKCδ, leading to eNOS phosphorylation at T495. Similarly, the overexpression of a T495D-eNOS mutant that mimics the phosphorylation at T495, was uncoupled, preferentially localized to the mitochondria, and disrupted mitochondrial bioenergetics, suggesting that eNOS phosphorylation at T495 is sufficient to mediate the mitochondrial effects of ET-1 in PAECs. It should be noted that other PKC isoforms may also be involved in ET-1–mediated pulmonary remodeling; for example, PKCα has been shown to participate in the ET-1–mediated pulmonary artery smooth muscle cell proliferation through the opening of calcium channels (38). In addition, the exposure of human umbilical vein endothelial cells to oxidized low-density lipoprotein, another eNOS uncoupler, results in increased phosphorylation of eNOS at T495, again by activating PKCα (20). ET-1 has also been suggested to induce a pulmonary vasoconstrictor response through PKCβ (39). Thus, just like the complex or even conflicting reports on the role of PKC in mediating myocardial protection from ischemia (40), ET-1–PKC interactions are complex. However, recent and growing evidence suggests that PKCδ may play the predominant role in ET-1–mediated constriction and blood pressure elevation (41, 42). Consistent with these studies, we found that a PKCδ-inhibitory peptide significantly attenuated ET-1–induced eNOS mitochondrial redistribution and preserved mitochondrial bioenergetics. Interestingly, the inhibition of PKCδ actually led to an increase in mitochondrial respiratory capacity. The reason for this is

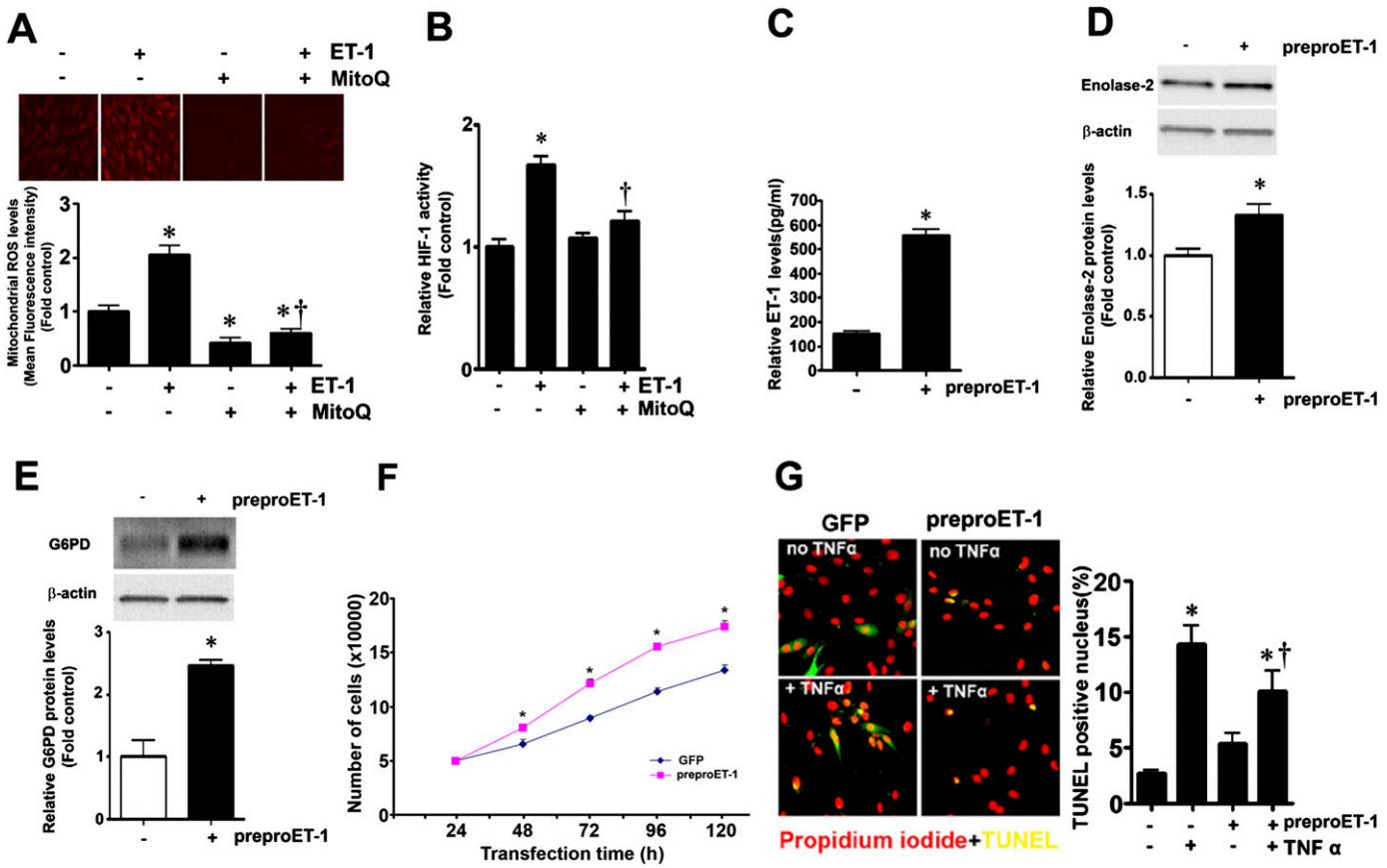

Figure 6. ET-1 induces a mitochondrial ROS–dependent increase in HIF-1 signaling in PAECs. PAECs were pretreated with MitoQ (100 nM) or control compound, decylTPP (100 nM), for 1 hour, followed ET-1 (100 nM, 4 h), and mitochondrial ROS levels and HIF-1 activity determined. MitoQ attenuated both the basal and ET-1–dependent increase in mitochondrial ROS generation in PAECs compared with decylTPP-treated cells (*A*). ET-1 increased the promoter activity of an HIF-1–dependent reporter (*B*), and this was attenuated in the presence MitoQ (*B*). PAECs were transfected with an expression plasmid for prepro-ET-1 or an empty pcDNA3 plasmid (as a control). After 48 hours, ET-1 levels in the culture medium were significantly higher in cells overexpressing prepro-ET-1 (*C*). Western blot analysis also revealed that prepro-ET1 overexpression increased the protein levels of enolase-2 (*D*) and glucose-6-phosphate dehydrogenase (G6PD) (*E*). Transfection with an expression plasmid for prepro-ET-1 significantly increased PAEC proliferation (*F*) and decreased the apoptotic cell death associated with exposure to TNF-α (*G*). Values are means ± SEM; n = 6–11. $^{*}P < 0.05$ versus control compound, decylTPP, treatment or control plasmid overexpression; $^{\dagger}P < 0.05$ versus ET-1 treatment or prepro-ET-1 overexpression.

unclear. However, recent studies suggest that PKCδ is capable of modulating mitochondrial function. For example, it has been shown that the attenuation of mitochondrial dehydrogenase activity, and the mitochondrial membrane potential correlates with increased PKCδ activity (43). Conversely, it has been reported that mitochondrial function is compromised in PKCδ knockout mice, which leads to an increased ROS generation and a shift from glucose to lipid metabolism in the heart (44).

Studies suggest that mitochondrial-derived ROS can serve as signaling molecules in glucose metabolism (45). Furthermore, increasing evidence indicates that ROS generated by mitochondria can stabilize HIF-1α, which can stimulate glycolytic energy production, at least in cancer cells, and HIF-1 has been implicated in regulating many of the genes that are responsible for glycolysis (reviewed in Ref. 22). It has also been recently shown that HIF-1α is involved in the switch from oxidative phosphorylation to glycolysis in endothelial cells during the development of PH (46). Consistent with these studies, our results indicate that ET-1 induced both HIF-1 activity and the expression of enolase-2 and G6PD, both of which are involved in glycolysis and are known to be regulated by HIF-1. Although our data did not allow us to determine the exact mechanism by which mitochondrial derived ROS, we can speculate. Previous studies have also shown that HIF-1 can increase ET-1 expression (47), whereas von Hippel-Lindau, an E3 ubiquitin ligase that modifies HIF-1α and targets it for degradation (reviewed in Ref. 22) is inhibited by ROS (48). Thus, it is possible that the increase in mitochondrial ROS induced by ET-1 leads to the inhibition of von Hippel-Lindau and the subsequent stabilization of HIF-1α, which could lead to a feed-forward signaling cascade in which increases in HIF-1 lead to more ET-1 generation. However, further studies will be required to test this possibility. It should be noted that there are likely other glycolysis-regulating genes that we did not examine that are either directly dependent on HIF-1 binding, as well as other genes that are independent of HIF-1α, but regulated by redox-sensitive transcription factors. For example, recent studies also indicate that redox-sensitive transcription factor, NF-κB,

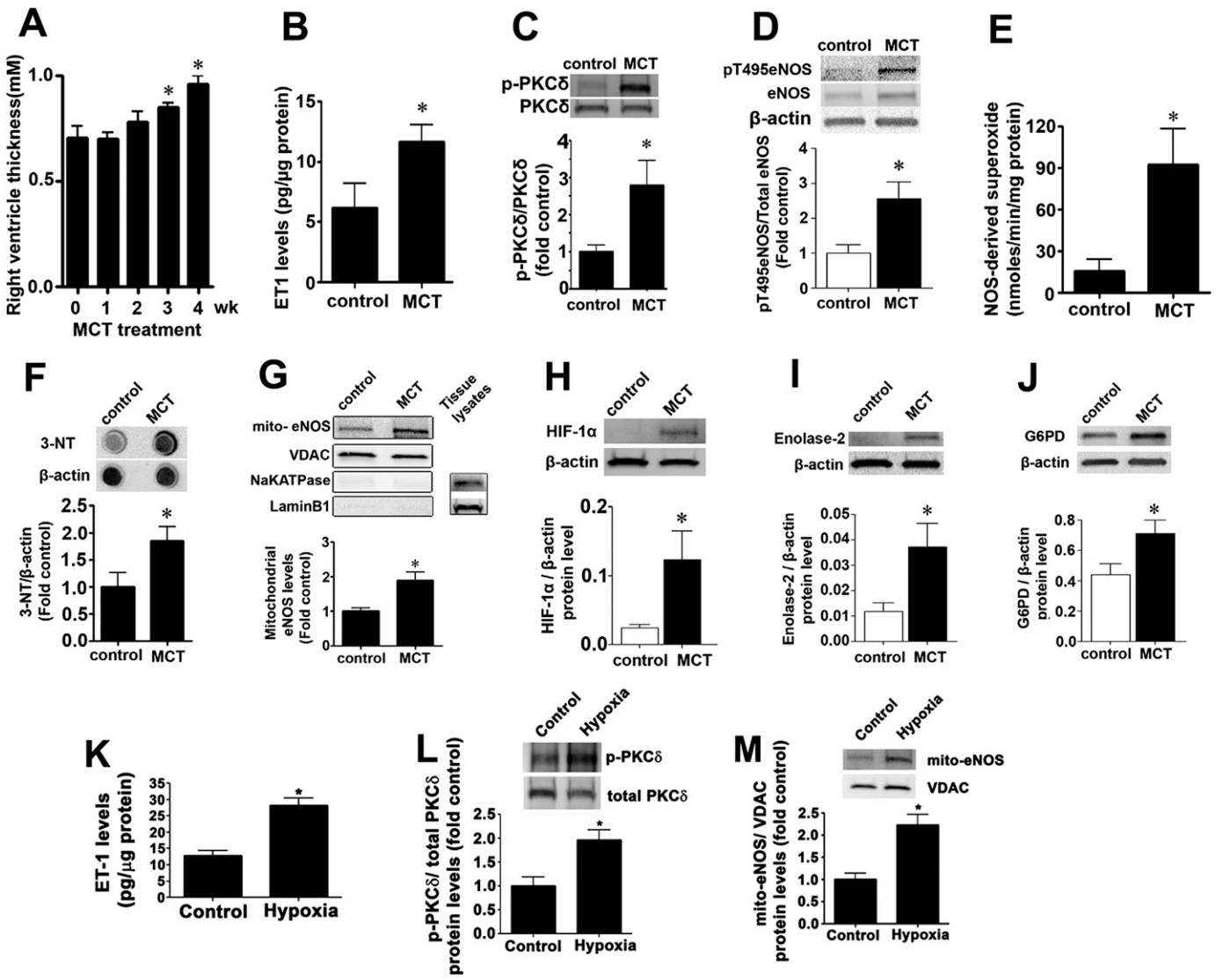

Figure 7. The mitochondrial translocation of eNOS is recapitulated in rodent models of pulmonary hypertension. Monocrotaline (MCT) treatment significantly increased right ventricle (RV) thickness in rats after 3 and 4 weeks (*A*). ET-1 levels were significantly increased in the MCT rat lung tissue (*B*). Western blot analysis, using whole-lung extracts, demonstrates that MCT treatment significantly increased PKCδ phosphorylation (*C*) and T495 eNOS phosphorylation (*D*). The increased eNOS phosphorylation at T495 in MCT rats correlates with increased NOS-derived superoxide (*E*) and total protein nitration (*F*). Lung mitochondrial protein extracts (5 μg) were also subjected to Western blotting using an antibody raised against eNOS. MCT treatment increased eNOS accumulation in the mitochondria (*G*). Loading was normalized by reprobing with the mitochondrial protein, VDAC (*G*), and reprobed with antibodies raised against NaKATPase, or laminB1 to demonstrate no cross-contamination with the plasma membrane, or nuclear fractions, respectively (*G*). Western blot analysis of whole-lung extracts indicates that MCT treatment increased HIF-1α (*H*), enolase-1 (*I*), and G6PD (*J*) protein levels ET-1 (*K*). PKCδ phosphorylation (*L*) and eNOS mitochondrial translocation (*M*) were also increased in mice exposed to chronic hypoxia. Values are means ± SEM; $n = 4–7$. $^*P < 0.05$ versus control.

is also involved in regulating glycolysis (49). activating protein-1 and specificity protein 1 are also redox sensitive and are involved in regulating the expression of lactate dehydrogenase, the product of which plays a pivotal role in the increase in glycolysis seen in human cancers (50).

Taken together, our data suggest that there is a link between increased ET-1 levels and the mitochondrial remodeling that occurs in PAECs during the development of PH. Furthermore, we have shown that this is mediated via PKCδ-dependent phosphorylation of eNOS at T495, increased eNOS uncoupling, and its mitochondrial redistribution. The resulting disruption of carnitine homeostasis results in a bioenergetic shift from oxidative phosphorylation to glycolysis. Thus, our study has elucidated a novel target for ET-1 in the development of PH, and suggests that pursuing mitochondrial-targeted therapies through the inhibition of PKCδ signaling may be an avenue for the treatment of PH. ■

Author disclosures are available with the text of this article at www.atsjournals.org.

References

1. Blomgren K, Zhu C, Hallin U, Hagberg H. Mitochondria and ischemic reperfusion damage in the adult and in the developing brain. *Biochem Biophys Res Commun* 2003;304:551–559.
2. O'Brien D, Chunduri P, Iyer A, Brown L. L-carnitine attenuates cardiac remodelling rather than vascular remodelling in deoxycorticosterone acetate-salt hypertensive rats. *Basic Clin Pharmacol Toxicol* 2009; 106:296–301.
3. Warburg O. On the origin of cancer cells. *Science* 1956;123:309–314.
4. Xu W, Koeck T, Lara AR, Neumann D, DiFilippo FP, Koo M, Janocha AJ, Masri FA, Arroliga AC, Jennings C, *et al*. Alterations of cellular bioenergetics in pulmonary artery endothelial cells. *Proc Natl Acad Sci USA* 2007;104:1342–1347.
5. Giaid A, Yanagisawa M, Langleben D, Michel RP, Levy R, Shennib H, Kimura S, Masaki T, Duguid WP, Stewart DJ. Expression of endothelin-1 in the lungs of patients with pulmonary hypertension. *N Engl J Med* 1993;328:1732–1739.
6. Rodrigo R, Gonzalez J, Paoletto F. The role of oxidative stress in the pathophysiology of hypertension. *Hypertens Res* 2011;34:431–440.
7. Rafikova O, Rafikov R, Kumar S, Sharma S, Aggarwal S, Schneider F, Jonigk D, Black SM, Tofovic SP. Bosentan inhibits oxidative and nitrosative stress and rescues occlusive pulmonary hypertension. *Free Radic Biol Med* 2013;56:28–43.
8. Oishi P, Azakie A, Harmon C, Fitzgerald RK, Grobe A, Xu J, Hendricks-Munoz K, Black SM, Fineman JR. Nitric oxide–endothelin-1 interactions after surgically induced acute increases in pulmonary blood flow in intact lambs. *Am J Physiol Heart Circ Physiol* 2006;290: H1922–H1932.
9. Kumar S, Oishi PE, Rafikov R, Aggarwal S, Hou Y, Datar SA, Sharma S, Azakie A, Fineman JR, Black SM. Tezosentan increases nitric oxide signaling via enhanced hydrogen peroxide generation in lambs with surgically induced acute increases in pulmonary blood flow. *J Cell Biochem* 2013;114:435–447.
10. Kelly LK, Wedgwood S, Steinhorn RH, Black SM. Nitric oxide decreases endothelin-1 secretion through the activation of soluble guanylate cyclase. *Am J Physiol Lung Cell Mol Physiol* 2004;286: L984–L991.
11. Sud N, Sharma S, Wiseman DA, Harmon C, Kumar S, Venema RC, Fineman JR, Black SM. Nitric oxide and superoxide generation from endothelial NOS: modulation by Hsp90. *Am J Physiol Lung Cell Mol Physiol* 2007;293:L1444–L1453.
12. Aggarwal S, Gross CM, Kumar S, Datar S, Oishi P, Kalkan G, Schreiber C, Fratz S, Fineman JR, Black SM. Attenuated vasodilatation in lambs with endogenous and exogenous activation of cGMP signaling: role of protein kinase G nitration. *J Cell Physiol* 2011;226:3104–3113.
13. Wiseman DA, Wells SM, Hubbard M, Welker JE, Black SM. Alterations in zinc homeostasis underlie endothelial cell death induced by oxidative stress from acute exposure to hydrogen peroxide. *Am J Physiol Lung Cell Mol Physiol* 2007;292:L165–L177.
14. Sharma S, Sud N, Wiseman DA, Carter AL, Kumar S, Hou Y, Rau T, Wilham J, Harmon C, Oishi P, *et al*. Altered carnitine homeostasis is associated with decreased mitochondrial function and altered nitric oxide signaling in lambs with pulmonary hypertension. *Am J Physiol Lung Cell Mol Physiol* 2008;294:L46–L56.
15. Brand MD, Nicholls DG. Assessing mitochondrial dysfunction in cells. *Biochem J* 2011;435:297–312.
16. Sun X, Sharma S, Fratz S, Kumar S, Rafikov R, Aggarwal S, Rafikova O, Lu Q, Burns T, Dasarathy S, *et al*. Disruption of endothelial cell mitochondrial bioenergetics in lambs with increased pulmonary blood flow. *Antioxid Redox Signal* 2012;18:1739–1752.
17. Radi R. Nitric oxide, oxidants, and protein tyrosine nitration. *Proc Natl Acad Sci USA* 2004;101:4003–4008.
18. Tian J, Hou Y, Lu Q, Wiseman DA, Vasconcelos Fonsesca F, Elms S, Fulton DJ, Black SM. A novel role for caveolin-1 in regulating endothelial nitric oxide synthase activation in response to H_2O_2 and shear stress. *Free Radic Biol Med* 2010;49:159–170.
19. Rafikov R, Rafikova O, Aggarwal S, Gross C, Sun X, Desai J, Fulton D, Black SM. Asymmetric dimethylarginine induces endothelial nitric-oxide synthase mitochondrial redistribution through the nitration-mediated activation of Akt1. *J Biol Chem* 2013;288:6212–6226.
20. Xie L, Liu Z, Lu H, Zhang W, Mi Q, Li X, Tang Y, Chen Q, Ferro A, Ji Y. Pyridoxine inhibits endothelial NOS uncoupling induced by oxidized low-density lipoprotein via the PKCα signalling pathway in human umbilical vein endothelial cells. *Br J Pharmacol* 2012;165:754–764.
21. Rafikov R, Fonseca FV, Kumar S, Pardo D, Darragh C, Elms S, Fulton D, Black SM. eNOS activation and no function: structural motifs responsible for the posttranslational control of endothelial nitric oxide synthase activity. *J Endocrinol* 2011;210:271–284.
22. Denko NC. Hypoxia, HIF1 and glucose metabolism in the solid tumour. *Nat Rev Cancer* 2008;8:705–713.
23. Piao L, Marsboom G, Archer SL. Mitochondrial metabolic adaptation in right ventricular hypertrophy and failure. *J Mol Med (Berl)* 2010;88: 1011–1020.
24. Gomez-Arroyo JG, Farkas L, Alhussaini AA, Farkas D, Kraskauskas D, Voelkel NF, Bogaard HJ. The monocrotaline model of pulmonary hypertension in perspective. *Am J Physiol Lung Cell Mol Physiol* 2012;302:L363–L369.
25. Finlay DK. Regulation of glucose metabolism in T cells: new insight into the role of phosphoinositide 3-kinases. *Front Immunol* 2012;3:247.
26. Rehman J, Archer SL. A proposed mitochondrial-metabolic mechanism for initiation and maintenance of pulmonary arterial hypertension in fawn-hooded rats: the Warburg model of pulmonary arterial hypertension. *Adv Exp Med Biol* 2010;661:171–185.
27. Wedgwood S, Dettman RW, Black SM. ET-1 stimulates pulmonary arterial smooth muscle cell proliferation via induction of reactive oxygen species. *Am J Physiol Lung Cell Mol Physiol* 2001;281:L1058–L1067.
28. Narayanan D, Xi Q, Pfeffer LM, Jaggar JH. Mitochondria control functional CaV1.2 expression in smooth muscle cells of cerebral arteries. *Circ Res* 2010;107:631–641.
29. Sethi AS, Lees DM, Douthwaite JA, Dawnay AB, Corder R. Homocysteine-induced endothelin-1 release is dependent on hyperglycaemia and reactive oxygen species production in bovine aortic endothelial cells. *J Vasc Res* 2006;43:175–183.
30. Lee KU, Lee IK, Han J, Song DK, Kim YM, Song HS, Kim HS, Lee WJ, Koh EH, Song KH, *et al*. Effects of recombinant adenovirus–mediated uncoupling protein 2 overexpression on endothelial function and apoptosis. *Circ Res* 2005;96:1200–1207.
31. Yuhki KI, Miyauchi T, Kakinuma Y, Murakoshi N, Maeda S, Goto K, Yamaguchi I, Suzuki T. Endothelin-1 production is enhanced by rotenone, a mitochondrial complex I inhibitor, in cultured rat cardiomyocytes. *J Cardiovasc Pharmacol* 2001;38:850–858.
32. Kakinuma Y, Miyauchi T, Yuki K, Murakoshi N, Goto K, Yamaguchi I. Novel molecular mechanism of increased myocardial endothelin-1 expression in the failing heart involving the transcriptional factor hypoxia-inducible factor-1alpha induced for impaired myocardial energy metabolism. *Circulation* 2001;103:2387–2394.
33. Masri FA, Xu W, Comhair SA, Asosingh K, Koo M, Vasanji A, Drazba J, Anand-Apte B, Erzurum SC. Hyperproliferative apoptosis–resistant endothelial cells in idiopathic pulmonary arterial hypertension. *Am J Physiol Lung Cell Mol Physiol* 2007;293:L548–L554.
34. Dranka BP, Hill BG, Darley-Usmar VM. Mitochondrial reserve capacity in endothelial cells: the impact of nitric oxide and reactive oxygen species. *Free Radic Biol Med* 2010;48:905–914.
35. Akundi RS, Zhi L, Sullivan PG, Bueler H. Shared and cell type–specific mitochondrial defects and metabolic adaptations in primary cells from PINK1-deficient mice. *Neurodegener Dis* 2013;12:136–149.
36. Gao S, Chen J, Brodsky SV, Huang H, Adler S, Lee JH, Dhadwal N, Cohen-Gould L, Gross SS, Goligorsky MS. Docking of endothelial nitric oxide synthase (eNOS) to the mitochondrial outer membrane: a pentabasic amino acid sequence in the autoinhibitory domain of eNOS targets a proteinase K–cleavable peptide on the cytoplasmic face of mitochondria. *J Biol Chem* 2004;279:15968–15974.
37. Sud N, Wells SM, Sharma S, Wiseman DA, Wilham J, Black SM. Asymmetric dimethylarginine inhibits Hsp90 activity in pulmonary arterial endothelial cells: role of mitochondrial dysfunction. *Am J Physiol Cell Physiol* 2008;294:C1407–C1418.
38. Lin YL, Lin RJ, Shen KP, Dai ZK, Chen IJ, Wu JR, Wu BN. Baicalein, isolated from *Scutellaria baicalensis*, protects against endothelin-1–induced pulmonary artery smooth muscle cell proliferation via inhibition of TRPC1 channel expression. *J Ethnopharmacol* 2011; 138:373–381.

39. Snow JB, Gonzalez Bosc LV, Kanagy NL, Walker BR, Resta TC. Role for PKCbeta in enhanced endothelin-1–induced pulmonary vasoconstrictor reactivity following intermittent hypoxia. *Am J Physiol Lung Cell Mol Physiol* 2011;301:L745–L754.
40. Chen L, Hahn H, Wu G, Chen CH, Liron T, Schechtman D, Cavallaro G, Banci L, Guo Y, Bolli R, *et al*. Opposing cardioprotective actions and parallel hypertrophic effects of delta PKC and epsilon PKC. *Proc Natl Acad Sci USA* 2001;98:11114–11119.
41. Webster BR, Osmond JM, Paredes DA, DeLeon XA, Jackson-Weaver O, Walker BR, Kanagy NL. Phosphoinositide-dependent kinase-1 and protein kinase Cdelta contribute to endothelin-1 constriction and elevated blood pressure in intermittent hypoxia. *J Pharmacol Exp Ther* 2013;344:68–76.
42. Choudhary G, Troncales F, Martin D, Harrington EO, Klinger JR. Bosentan attenuates right ventricular hypertrophy and fibrosis in normobaric hypoxia model of pulmonary hypertension. *J Heart Lung Transplant* 2011;30:827–833.
43. Lai HC, Yeh YC, Wang LC, Ting CT, Lee WL, Lee HW, Wang KY, Wu A, Su CS, Liu TJ. Propofol ameliorates doxorubicin-induced oxidative stress and cellular apoptosis in rat cardiomyocytes. *Toxicol Appl Pharmacol* 2011;257:437–448.
44. Mayr M, Chung YL, Mayr U, McGregor E, Troy H, Baier G, Leitges M, Dunn MJ, Griffiths JR, Xu Q. Loss of PKC-delta alters cardiac metabolism. *Am J Physiol Heart Circ Physiol* 2004;287:H937–H945.
45. Sena LA, Chandel NS. Physiological roles of mitochondrial reactive oxygen species. *Mol Cell* 2012;48:158–167.
46. Fijalkowska I, Xu W, Comhair SA, Janocha AJ, Mavrakis LA, Krishnamachary B, Zhen L, Mao T, Richter A, Erzurum SC, *et al*. Hypoxia inducible-factor1alpha regulates the metabolic shift of pulmonary hypertensive endothelial cells. *Am J Pathol* 2010;176:1130–1138.
47. Yamashita K, Discher DJ, Hu J, Bishopric NH, Webster KA. Molecular regulation of the endothelin-1 gene by hypoxia: contributions of hypoxia-inducible factor-1, activator protein-1, GATA-2, and p300/CBP. *J Biol Chem* 2001;276:12645–12653.
48. Bell EL, Klimova TA, Eisenbart J, Schumacker PT, Chandel NS. Mitochondrial reactive oxygen species trigger hypoxia-inducible factor–dependent extension of the replicative life span during hypoxia. *Mol Cell Biol* 2007;27:5737–5745.
49. Martinez-Outschoorn UE, Curry JM, Ko YH, Lin Z, Tuluc M, Cognetti D, Birbe RC, Pribitkin E, Bombonati A, Pestell RG, *et al*. Oncogenes and inflammation rewire host energy metabolism in the tumor microenvironment: Ras and NFkB target stromal MCT4. *Cell Cycle* 2013;12:2580–2597.
50. Jungmann RA, Huang D, Tian D. Regulation of LDH-A gene expression by transcriptional and posttranscriptional signal transduction mechanisms. *J Exp Zool* 1998;282:188–195.